JOURNAL OF APPLIED PHYSICS **114**, 104104 (2013)

# Computational model of deformable lenses actuated by dielectric elastomers

Tongqing Lu,[1,2] Shengqiang Cai,[3] Huiming Wang,[2,4] and Zhigang Suo[2,a)]
[1]*State Key Lab for Strength and Vibration of Mechanical Structures, International Center of Applied Mechanics, School of Aerospace Engineering, Xi'an Jiaotong University, Xi'an 710049, China*
[2]*School of Engineering and Applied Sciences, Harvard University, Cambridge, Massachusetts 02138, USA*
[3]*Department of Mechanical and Aerospace Engineering, Jacobs School of Engineering, University of California, San Diego, California 92093, USA*
[4]*Department of Engineering Mechanics, Zhejiang University, Hangzhou 310027, China*

(Received 19 July 2013; accepted 26 August 2013; published online 12 September 2013)

A recent design of deformable lens mimics the human eye, adjusting its focal length in response to muscle-like actuation. The artificial muscle is a membrane of a dielectric elastomer subject to a voltage. Here, we calculate the coupled and inhomogeneous deformation of the lens and the dielectric elastomer actuator by formulating a nonlinear boundary-value problem. We characterize the strain-stiffening elastomer with the Gent model and describe the voltage-induced deformation using the model of ideal dielectric elastomer. The computational predictions agree well with experimental data. We use the model to explore the space of parameters, including the prestretch of the membrane, the volume of the liquid in the lens, and the size of the dielectric elastomer actuator relative to the lens. We examine how various modes of failure limit the minimum radius of curvature. © *2013 AIP Publishing LLC*. [http://dx.doi.org/10.1063/1.4821028]

## I. INTRODUCTION

The worldwide adoption of mobile phones has highlighted a challenge: zooming—a rigid-body translation—requires large space, and is unsuitable for cameras on mobile phones. A potential solution is to mimic the human eye and make the lens deformable. A recent design of deformable lens comprises two layers of a prestretched dielectric elastomer (Fig. 1).[1] The annular part is sandwiched between conformal electrodes, and acts as an artificial muscle. The inner part encloses a transparent liquid and acts as a lens. When a voltage is applied between the electrodes, the dielectric elastomer actuator expands and the lens deforms, adjusting its focal length. Although deformable lenses actuated by other means are being explored,[2,3] deformable lenses actuated by dielectric elastomers have several attributes, such as compact structure, light weight, quietness, and low power.

The emergence of dielectric elastomers[4–7] promises muscle-like transducers for broad range of applications, including actuators and sensors in robotics, prosthetics, optics, and haptics.[8–12] Also under development are generators for harvesting energy from human movements and ocean waves.[13–15] The achievable voltage-induced deformation of dielectric elastomers depends on how mechanical loads are applied.[16] Using an acrylic elastomer, experiments have demonstrated voltage-induced expansion in area by 158% with a membrane biaxially prestretched and fixed to a rigid frame,[4] by 260% with a clamped membrane,[17] by 488% with a membrane subject to biaxial dead loads,[18] and by 1689% with a membrane mounted on a chamber of air.[19] The large deformation may be accompanied with rich nonlinear behavior of instability, which can be harnessed to enhance dramatically the performance of transducers.[20,21] The membranes may even exhibit electromechanical phase transition.[22–24] The development of the theory of dielectric elastomers presents an unique opportunity in mechanics.[25]

This paper presents a computational model to aid the further development of dielectric elastomer lenses. We calculate the inhomogeneous deformation in the lens and the dielectric elastomer actuator by formulating a nonlinear boundary-value problem. We represent the strain-stiffening elastomer with the Gent model[26] and describe the voltage-induced deformation using the model of ideal dielectric elastomers.[22] We compare computational results with experimental data. The model enables us to explore the space of a large number of parameters, such as the prestretch, the volume of the liquid, and the size of the dielectric elastomer actuator. We examine how various modes of failure limit the minimal radius of curvature.

## II. GOVERNING EQUATIONS

We formulate governing equations for the dielectric elastomer actuator and the lens separately. We then make the displacement and force continuous at the boundary between the actuator and the lens. So far, no model has dealt with dielectric elastomer lenses. Several groups have developed finite element methods for dielectric elastomer actuators.[27–32] Here, we adapt a specialized numerical method taking advantage of axisymmetric shape of the curved membranes.[33–36] We focus on the dielectric elastomer lens described in Ref. 1, although the method of analysis can be used to model other designs of dielectric elastomer lenses.[37]

The deformable lens can be in several states. In the reference state, Fig. 1(a), subject to no force or voltage, the membrane is undeformed. The inside circular part corresponds to the lens, radius $A$, and thickness $H$. The annular part corresponds to the dielectric elastomer actuator of outer radius $B$ and is sandwiched between conformal electrodes. In

a)Author to whom correspondence should be addressed. Email: suo@seas.harvard.edu

 

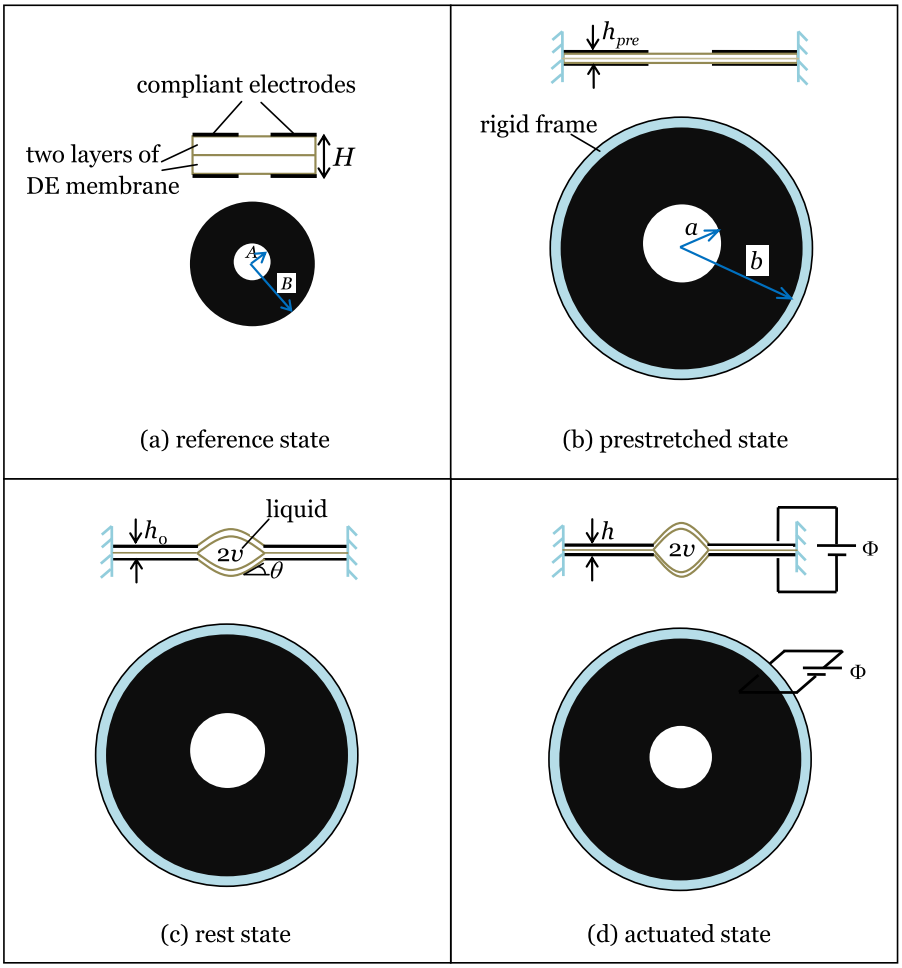


FIG. 1. Schematics of the deformable lens in successive states. (a) Reference state in which the membrane is subject to no force or voltage. (b) Prestretched state in which the membrane is pre-stretched homogeneously and fixed to a rigid frame. (c) Rest state in which the liquid is injected into the lens. (4) Actuated state in which the curvature of the lens changes with the voltage applied to the dielectric elastomer actuator.

the prestretched state, Fig. 1(b), the whole membrane is stretched homogeneously and fixed to a rigid frame. The inner radius becomes $a$, and the outer radius $b$. In the rest state, Fig. 1(c), an incompressible liquid of volume $2v$ is injected into the passive part, the radius of which becomes $a_{rest}$. The apex of the lens reaches the height $w_0$ off the middle plane, and the pressure in the liquid relative to the pressure in the ambient is $p_0$. Let $\rho_0$ be the radius of curvature at the apex in the rest state. The dielectric elastomer actuator remains being flat. In the actuated state, Fig. 1(d), the dielectric elastomer actuator is subject to a voltage $\Phi$, expanding area in the plane and decreasing its thickness to $h$. As a result, the lens is squeezed so that the radius of curvature at the apex changes to $\rho$.

The device is symmetric with respect to the middle plane, so we only consider one layer of the membrane in the calculation. In the reference state, Fig. 1(a), label each material particle in the lens by its radial co-ordinated $R$ in the interval $(0, A)$. In the subsequent states, Figs. 1(b)–1(d), the lens deforms into axisymmetric shapes. Let the co-ordinate $r$ coincide with a radial direction, the co-ordinate $z$ coincide with the axis of symmetry, and the plane $z = 0$ coincide with the middle plane. In a deformed state, the material particle $R$ takes the position of co-ordinates $z$ and $r$. The functions $z(R)$ and $r(R)$ characterize the deformed state of the membrane.

Consider a differential material element between two material particles $R$ and $R + dR$. When the membrane is in a deformed state, the particle $R$ takes the position of co-ordinates $z(R)$ and $r(R)$, while the particle $R + dR$ takes the position of co-ordinates $z(R + dR)$ and $r(R + dR)$. In the undeformed state, the material element is a straight segment, length $dR$. In the deformed state, the material element becomes a curved segment of length $\lambda_1 dR$, where $\lambda_1$ is the longitudinal stretch. In a deformed state, let $\theta(R)$ be the slope of a membrane at material particle $R$. Write $dr = r(R + dR) - r(R)$, so that

$$\frac{dr}{dR} = \lambda_1 \cos\theta. \tag{1}$$

Similarly, write $dz = z(R + dR) - z(R)$, so that

$$\frac{dz}{dR} = -\lambda_1 \sin\theta. \tag{2}$$

Consider in the undeformed state a circle of material particles, perimeter $2\pi R$. In the deformed state, these material particles occupy a circle of positions, perimeter $2\pi r$. The deformation causes the latitudinal stretch $\lambda_2 = r/R$. When the membranes are in the pre-stretched state, Fig. 1(b), both stretches are homogeneous in the membranes, $\lambda_1 = \lambda_2 = a/A$. When the membranes are in a curved state, Figs. 1(c) and 1(d), however, the stretches are inhomogeneous in the membranes and are described by functions $\lambda_1(R)$ and $\lambda_2(R)$. The volume enclosed by

the curved membrane and the middle plane is $v = \int_0^a 2\pi z r dr$.

The conditions of equilibrium are (Appendix A)

$$\frac{d}{dR}\left(\frac{H}{2}Rs_1 \sin\theta\right) = \lambda_1\lambda_2 Rp\cos\theta, \tag{3}$$

$$\frac{d}{dR}\left(\frac{H}{2}Rs_1 \cos\theta\right) - \frac{H}{2}s_2 = \lambda_1\lambda_2 Rp\sin\theta, \tag{4}$$

where the nominal stresses are given by

$$s_1 = \frac{\partial W_{stretch}(\lambda_1,\lambda_2)}{\partial\lambda_1}, \quad s_2 = \frac{\partial W_{stretch}(\lambda_1,\lambda_2)}{\partial\lambda_2}. \tag{5}$$

Here $W_{stretch}(\lambda_1,\lambda_2)$ is the density Helmholtz free energy of the elastomer.

At the apex of the lens, $R = 0$, symmetry requires that

$$\theta(0) = 0, \quad r(0) = 0. \tag{6}$$

At the boundary of connection, $R = A$, the membrane is connected to the middle plane

$$z(A) = 0, \tag{7}$$

and the displacement and force is continuous with those of the dielectric elastomer actuator

$$(s_1\cos\theta)|_A = s_{conti}, \quad r(A) = r_{conti}. \tag{8}$$

In the reference state, Fig. 1(a), label each material particle in the dielectric elastomer actuator by its radial coordinated $R$ in the interval $(A, B)$. In the deformed states, Figs. 1(b)–1(d), the dielectric elastomer actuator remains flat, and the material particle $R$ takes position of radius $r$. The function $r(R)$ describes the deformed state of the dielectric elastomer actuator. The radial stretch is $\lambda_1 = dr/dR$, and the hoop stretch $\lambda_2 = r/R$. The charge on the membrane is $Q = \int_A^B 2\pi D r dr$, where $D$ is the electrical displacement. The electrical field relates to the voltage as $E = \Phi/h$. The conditions of equilibrium are (Appendix B)

$$\frac{ds_1}{dR} - \frac{s_2 - s_1}{R} = 0, \tag{9}$$

$$\frac{\partial W(\lambda_1,\lambda_2,D)}{\partial D} = E. \tag{10}$$

Here, we have additional variable $D$ in the density Helmholtz free energy of the dielectric elastomer $W(\lambda_1,\lambda_2,D)$, because the dielectric elastomer stores both stretching energy and electrostatic energy upon electrical loading. The nominal stresses are given by

$$s_1 = \frac{\partial W(\lambda_1,\lambda_2,D)}{\partial\lambda_1} - \frac{\Phi}{H}D\lambda_2, \quad s_2 = \frac{\partial W(\lambda_1,\lambda_2,D)}{\partial\lambda_2} - \frac{\Phi}{H}D\lambda_1. \tag{11}$$

The outer boundary of the dielectric elastomer actuator is fixed to the rigid frame, so that

$$r(B) = b. \tag{12}$$

The inner boundary of the dielectric elastomer actuator is continuous with the lens, so that

$$s_1(A) = s_{conti}, \quad r(A) = r_{conti}. \tag{13}$$

## III. MATERIAL MODEL

To prescribe a specific form of the free energy function $W(\lambda_1,\lambda_2,D)$, we adopt the model of ideal dielectric elastomers.[22] This model assumes that the dielectric behavior of the elastomer is liquid-like, unaffected by deformation. This assumption is motivated as follows. An elastomer is a three-dimensional network of long and flexible polymers, held together by crosslinks. Each polymer chain consists of a large number of monomers. Consequently, the crosslinks negligibly affect the polarization of the monomers—that is, the elastomer can polarize nearly as freely as a polymer melt. The electric displacement $D$ is linear in the electric field $E$

$$D = \varepsilon E \tag{14}$$

with the permittivity $\varepsilon$ being independent of the stretches. Furthermore, the elastomer is assumed to be incompressible, so that the stretch in the thickness direction of the membrane, $\lambda_3$, related to $\lambda_1$ and $\lambda_2$ as $\lambda_3 = 1/\lambda_1\lambda_2$.

Inserting (14) into (10) and integrating with respect to $D$, we obtain that

$$W(\lambda_1,\lambda_2,D) = W_{stretch}(\lambda_1,\lambda_2) + \frac{D^2}{2\varepsilon}, \tag{15}$$

The constant of integration, $W_{stretch}(\lambda_1,\lambda_2)$, represents the free energy associated with the stretching of the elastomer. Equation (15) is readily interpreted. In the model of ideal dielectric elastomers, the free energy of the elastomer is the sum of that due to stretching the network and that due to polarization.

In an elastomer, each individual polymer chain has a finite contour length. When the elastomer is subject to no loads, the polymer chains are coiled, allowing a large number of conformations. Subject to loads, the polymer chains become less coiled. As the loads increase, the end-to-end distance of each polymer chain approaches the finite contour length, and the elastomer approaches a limiting stretch. On approaching the limiting stretch, the elastomer stiffens steeply. To account for this behavior, we adopt the Gent model[26]

$$W_{stretch}(\lambda_1,\lambda_2) = -\frac{\mu}{2}J_{\lim}\log\left(1 - \frac{\lambda_1^2 + \lambda_2^2 + \lambda_1^{-2}\lambda_2^{-2} - 3}{J_{\lim}}\right), \tag{16}$$

where $\mu$ is the shear modulus, and $J_{\lim}$ is a material constant related to the limiting stretch. When the stretches are small, $\lambda_1^2 + \lambda_2^2 + \lambda_1^{-2}\lambda_2^{-2} - 3 \ll J_{\lim}$, the Gent model recovers the neo-Hookean model, $W_{stretch}(\lambda_1,\lambda_2) = (\mu/2)(\lambda_1^2 + \lambda_2^2 + \lambda_1^{-2}\lambda_2^{-2} - 3)$. When the stretches approach the limit,

$\lambda_1^2+\lambda_2^2+\lambda_1^{-2}\lambda_2^{-2}-3\to J_{\lim}$, the Gent model stiffens steeply.

## IV. NOTES ON COMPUTATION

The governing equations in Sec. II result in a set of first-ordinary differential equations. The lens requires four functions: $\lambda_1(R), r(R), \theta(R), z(R)$. Equations (1) and (2) are in desired form. Equations (3) and (4), along with the material model in Sec. III, can be rewritten as

$$\frac{d\theta}{dR}=-\frac{s_2}{s_1}\frac{\sin\theta}{R}+\frac{\lambda_1\lambda_2}{s_1}\frac{2p}{H}, \tag{17}$$

$$\frac{d\lambda_1}{dR}=\frac{s_2\cos\theta-s_1+\frac{ds_1}{d\lambda_2}(\lambda_2-\lambda_1\cos\theta)}{R\frac{ds_1}{d\lambda_1}}. \tag{18}$$

Consequently, the lens is governed by four differential Eqs. (1), (2), (17), and (18), three boundary conditions (6) and (7), and two conditions of continuity (8).

The dielectric elastomer actuator requires two functions: $\lambda_1(R), \lambda_2(R)$. Rewritten Eq. (9) with respect to material model as

$$\frac{d\lambda_1}{dR}=\frac{s_2-s_1+\frac{ds_1}{d\lambda_2}(\lambda_2-\lambda_1)}{R\frac{ds_1}{d\lambda_1}}, \tag{19}$$

First order derivative of $\lambda_2(R)$ gives

$$\frac{d\lambda_2}{dR}=\frac{\lambda_1-\lambda_2}{R}, \tag{20}$$

Consequently, the dielectric elastomer actuator is governed by two differential Eqs. (19) and (20), one boundary condition (12) and two conditions of continuity (13).

The liquid is taken to be incompressible. As the lens deforms, the volume of the liquid enclosed in the lens remains constant at a prescribed value $2v$, while the pressure $p$ in the liquid needs to be calculated. In the calculation, however, we prescribe a pressure $p$ and the displacement at the connected boundary $r(A)$, and solve the boundary-value problems governing the lens and the dielectric elastomer actuator. The solution allows us to calculate a volume of the liquid and the stresses in the lens and artificial at their connection. We vary the pressure $p$ and the displacement $r(A)$ until the volume of the liquid equals the prescribed value $2v$, and the forces balance at the connection between the lens and the muscle, $(s_1\cos\theta)_{lens}=(s_1)_{muscle}$ at $R=A$.

## V. COMPUTATIONAL RESULTS AND DISCUSSIONS

We first compare the computational results with the experimental data extracted from Ref. 1. The parameters reported in the experiment and also used in the calculations are as follows. In the undeformed state, the thickness of the VHB4905 membrane is $H/2=0.5\,\text{mm}$, the outer radius is $B=5.25\,\text{mm}$, and the ratio between outer radius and inner radius is $B/A=2.76$. In the pre-stretched state, the pre-stretch is $b/B=4$. In the rest state, the radius of the lens is $a_{rest}=3.8\,\text{mm}$. The volume of liquid in the upper cap is $v=8.5\,\text{mm}^3$.

In the actuated state, as the voltage ramps up, the diameter of the lens decreases (Fig. 2). The computational results agree very well with the experimental data. The stretch in the experiment is far less than the limiting stretch of VHB4905, so that the calculation is insensitive to the value of $J_{\lim}$; we set a representative value $J_{\lim}=120$ throughout the paper.[16] Consequently, the only adjustable parameter in the calculation is $\sqrt{\mu/\varepsilon}$, which is found to be $2.84\times10^7\,\text{V/m}$ for the calculated diameters of the lens to best fit the experimental values. The representative value of permittivity is $\varepsilon=3.98\times10^{-11}\text{F/m}$,[38] which gives the shear modulus $\mu=32\,\text{kPa}$. This value of shear modulus slightly differ from that reported in the literature due to vicous effects.[18]

We consider two modes of failure: loss of tension and electrical breakdown. As the voltage ramps up, the dielectric elastomer actuator relaxes. At a certain voltage, the hoop stress vanishes at the outer boundary of the dielectric elastomer actuator. We mark the calculated point of loss of tension by the red circular dot (Fig. 2). In an actuated state, the deformation in the dielectric elastomer actuator is inhomogeneous, the thickness of the membrane varies from point to point, and the electric field is highest at the outer boundary of the dielectric elastomer actuator. We set a constant electrical breakdown strength $E_{EB}=200\,\text{MV/m}$,[16] and mark the calculated condition of electrical breakdown by a red cross (Fig. 2). The experiment is conservative: the applied voltage is well below the values that may cause loss of tension and electrical breakdown.

Beyond the loss of tension, the membrane is expected to form wrinkles. Our model, however, assumes that the membrane remains flat and sustains compression. Consequently, beyond the loss of tension, our model cannot predict the behavior of the wrinkled membrane, but give unstable equilibrium states assuming that the flat membrane remains flat.

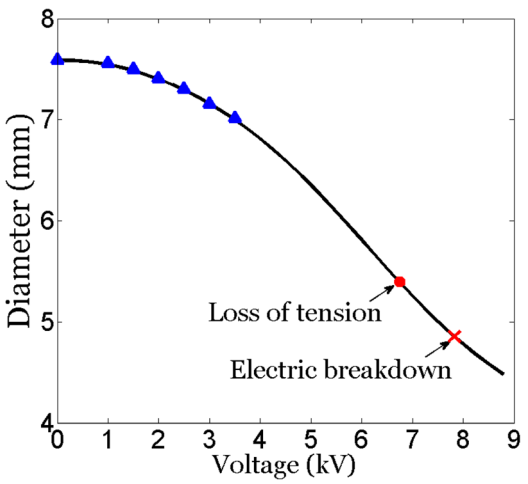


FIG. 2. The comparison between the experimental data and computational results. The blue triangles are the experimental data extracted from Ref. 1, while the black curve represents the computational results. The red circular dot corresponds to loss of tension. The red cross corresponds to electrical breakdown.

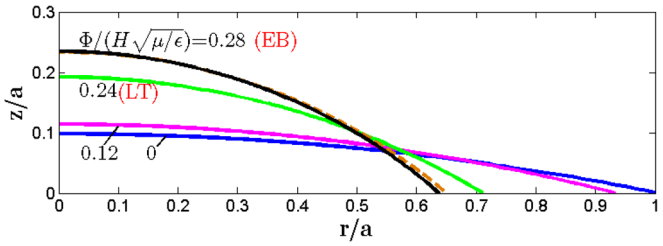


FIG. 3. Calculated shapes of the lens at several levels of voltage. The dashed curve represents the spherical cap of the same radius as the radius of curvature at the apex.

In particular, in Fig. 2, the solid line beyond the voltage causing the loss of tension is not a valid prediction of the diameter of the apex. The same caution applies to Figures 3–5. In all these figures, useful solutions should stay within the regime where the membrane remains in tension. We also include some unstable solutions corresponding flat membranes in compression, which will serve as a basis for comparison when future interest arises to develop solutions for wrinkled membranes.

As the voltage ramps up, the lens changes its shape, decreasing the diameter, and increasing the height (Fig. 3). We normalize the voltage as $\Phi/(H\sqrt{\mu/\varepsilon})$ in calculations. The labels LT and EB indicate loss of tension and electrical breakdown. Also included is the dashed curve, which represents the spherical cap of the same radius as the radius of curvature at the apex. This comparison indicates that taking the shape of the membrane as a spherical cap to calculate the size is a reasonable first approximation. A benefit of our model, however, is that the exact shape of the lens is computed. Instead of assuming a spherical lens, the exact aberrations and hence optical performance can be computed, which is of significant practical use.

The deformation of the membrane of the lens is inhomogeneous (Fig. 4). The differences of quantities in radial direction and latitudinal direction are small, especially when the muscle is under a low voltage. The inhomogeneity in the dielectric elastomer actuator is much more pronounced

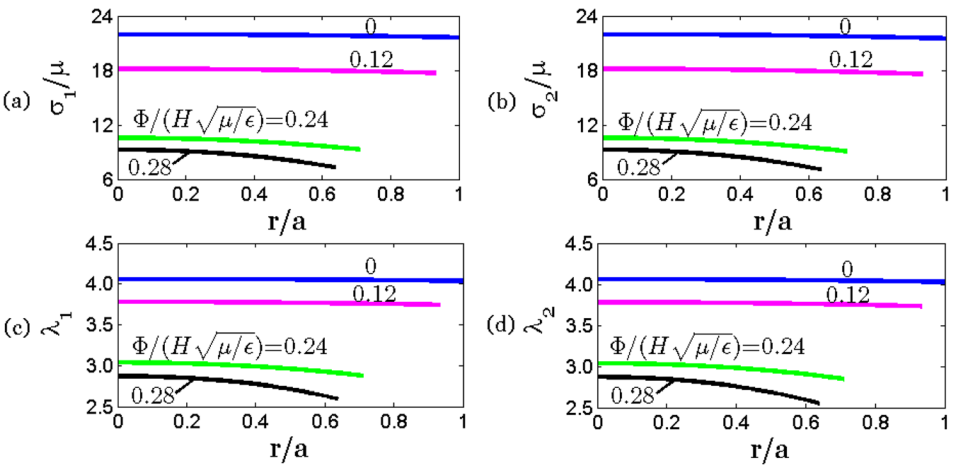


FIG. 4. Distributions of various quantities in the membrane of the lens at several levels of voltage. (a) Radial stress. (b) Hoop stress. (c) Radial stretch. (d) Hoop stretch.

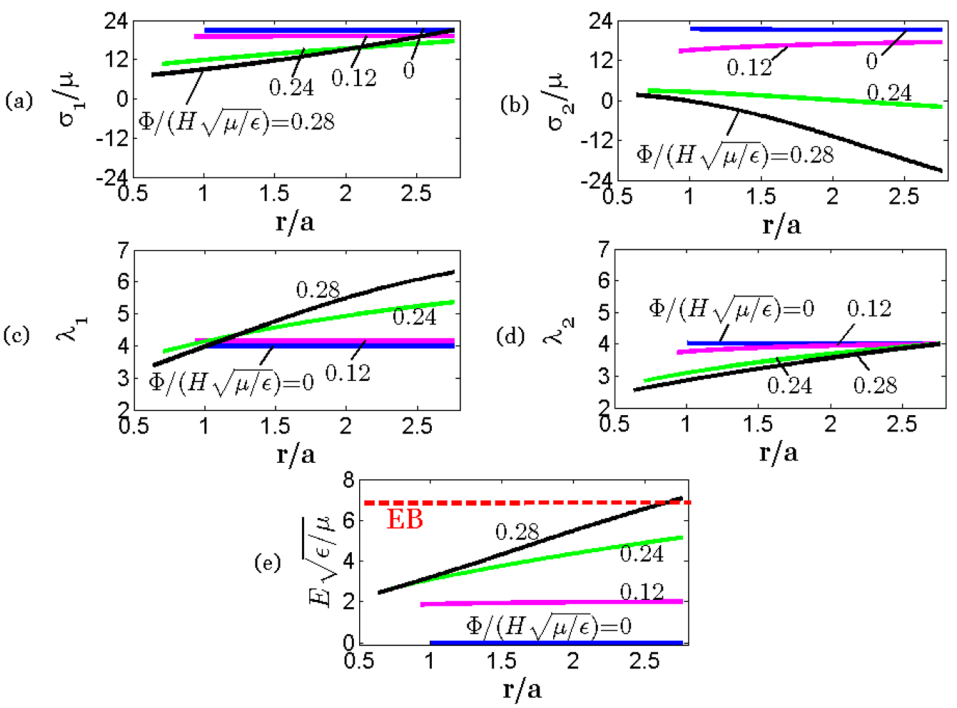


FIG. 5. Distributions of various quantities in the dielectric elastomer actuator at several levels of voltage. (a) Radial stress. (b) Hoop stress. (c) Radial stretch. (d) Hoop stretch. (e) Electric field.

(Fig. 5). In particular, the hoop stress is inhomogeneous in the actuator (Fig. 5(b)). Before the voltage is applied, $\Phi/(H\sqrt{\mu/\varepsilon}) = 0$, the hoop stress in the actuator is slightly inhomogeneous due to the additional pulling caused by the injection of the liquid into the lens. In this state, the hoop stress at the inner boundary of the actuator is slightly lower than that at the outer boundary. When the applied voltage is large, say, $\Phi/(H\sqrt{\mu/\varepsilon}) = 0.28$, the voltage causes the membrane to reduce the thickness and expands in area. At the inner boundary, the lens represents a spring-like boundary condition, and the stretch in both the radial and hoop directions can increase. At the outer boundary, however, the rigid frame allows the radial stretch to increase, but keeps the hoop stretch fixed. Consequently, when the effect of voltage prevails, the hoop stress at the inner boundary of the actuator is higher than that at the outer boundary. The loss of tension first occurs at the outer edge at the threshold voltage about $\Phi/(H\sqrt{\mu/\varepsilon}) = 0.237$. We use two significant digits throughout the paper, so that in the Fig. 5(b), we plot the curve at $\Phi/(H\sqrt{\mu/\varepsilon}) = 0.24$, where loss of tension already happens at the outer boundary and extends towards the inner boundary. The electric field at the outer boundary exceeds the electrical breakdown strength at the normalized voltage of $\Phi/(H\sqrt{\mu/\varepsilon}) = 0.28$ (Fig. 5(e)).

We characterize the performance of the lens by studying how the radius of curvature at the apex of the lens decreases as the voltage ramps up (Fig. 6). A steeply descending curve indicates a large change in the radius of curvature for a given voltage. Each curve terminates by a mode of failure, which we take to be either loss of tension or electrical breakdown. The characteristic curve depends on the values of the design parameters, such as the prestretch $b/B$, the volume of the liquid $v/a^3$, and the size of the dielectric elastomer actuator $B/A$. In each figure of (a)–(c), we fix two of the design parameters and vary the third. As the prestretch increases to an intermediate value (around 4), the maximum change of the radius of curvature increases (Fig. 6(a)). At larger prestretch, the improvement on actuation is limited. At a very large prestretch $b/B = 6$, the maximum actuation drops sharply, caused by electrical breakdown. The characteristic curve also depends on the volume of the liquid (Fig. 6(b)). One can choose a volume of liquid to satisfy a specific functional requirement. For example, in the experiment, the volume of liquid is chosen such that the curvature changes in the range similar to that of human eyes.[1] The improvement of the maximum actuation is quite limited with a much larger size of muscle (Fig. 6(c)). The value $B/A \sim 3$ is appropriate, which makes the device compact.

The maximum absolute actuation $\rho_{min}/a$ and the maximum relative actuation $\rho_{\min}/\rho_0$ are presented in Tables I and II, with different combinations of prestretch $b/B$ and volume of liquid $v/a^3$ and a fixed value of the size of dielectric elastomer actuator $B/A$. Bolditalic data points represent maximum actuation limited by electric breakdown, while the others represent maximum actuation limited by loss of tension. The absolute actuation determines the range that the deformable lens can undergo while the relative actuation reflects the deforming capability. For instance, the focal length of a lens can change from 100 m to 110 m, the absolute change 10 m is large but the stretching is only 110/100=1.1; on the contrast, a lens with focal length changing from 2 m to 4 m have higher deforming capability but shorter range. The absolute actuation and relative actuation of the deformable lens independently vary with the variable

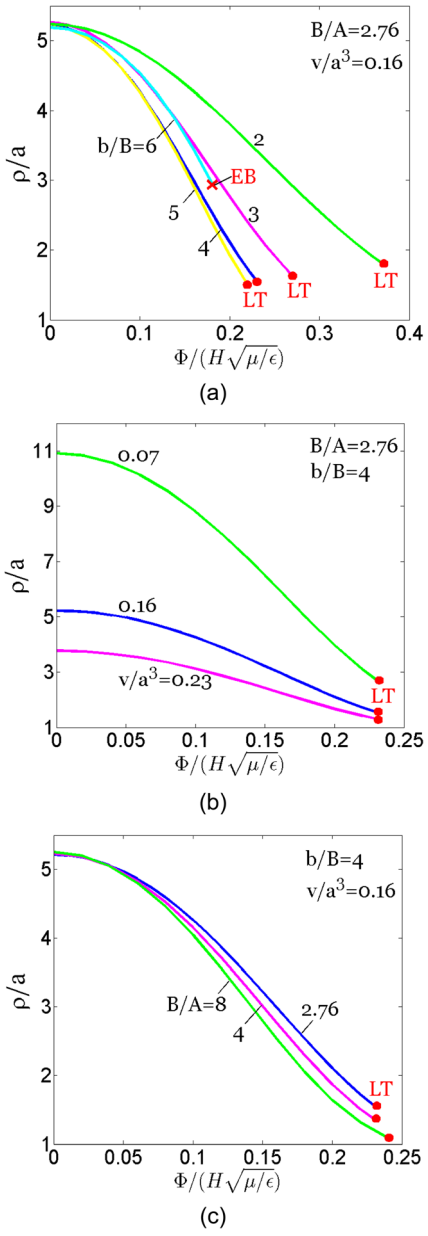


FIG. 6. The radius of curvature at the apex of the lens as a function of the applied voltage. (a) Effect of prestretch, $b/B$. (b) Effect of the volume of the liquid, $v/a^3$. (c) Effect of the size of the dielectric elastomer actuator, $B/A$.

TABLE I. Absolute change of radius of curvature at the apex $\rho_{\min}/a$with different combinations of prestretch $b/B$and volume of liquid $v/a^3$. The size of the dielectric elastomer actuator is $B/A = 2.76$.

| | Absolute change of radius of curvature $\rho_{\min}/a$ | | | | |
|---|---|---|---|---|---|
| Volume $v/a^3$ | $b/B$=2 | $b/B$=3 | $b/B$=4 | $b/B$=5 | $b/B$=6 |
| 0.07 | 3.35 | 3.14 | 2.72 | 2.67 | ***6.03*** |
| 0.16 | 1.81 | 1.63 | 1.56 | 1.51 | ***2.95*** |
| 0.22 | 1.38 | 1.34 | 1.30 | 1.24 | ***2.20*** |

TABLE II. Relative change of radius of curvature at the apex $\rho_{min}/\rho_0$ with different combinations of prestretch $b/B$ and volume of liquid $v/a^3$. The size of the dielectric elastomer actuator is $B/A = 2.76$.

| | Relative change of radius of curvature $\rho_{min}/\rho_0$ | | | | |
|---|---|---|---|---|---|
| Volume $v/a^3$ | $b/B$=2 | $b/B$=3 | $b/B$=4 | $b/B$=5 | $b/B$=6 |
| 0.07 | 0.31 | 0.29 | 0.25 | 0.24 | ***0.55*** |
| 0.16 | 0.34 | 0.31 | 0.30 | 0.29 | ***0.57*** |
| 0.22 | 0.37 | 0.36 | 0.34 | 0.33 | ***0.59*** |

parameters. For example, as the volume increases, the maximum absolute actuation decreases for a given prestretch while the maximum relative actuation increases.

Our computational model can aid the designers of tunable lenses. For the particular type of tunable lenses that mimic human eyes, our calculations and the above discussions indicate optimal parameters: prestretch around $b/B = 4$, volume of liquid $v/a^3$=0.16, and the size of the dielectric elastomer actuator around $B/A$=3. These parameters are close to those used in the experiment in Ref. 1. The large prestretch of 4 keeps the membrane in tension during actuation, and lowers the voltage needed for actuation. The size of the dielectric elastomer actuator reflects a compromise to ensure the performance of the lens and keep the whole device compact. Given this choice of parameters, our calculation indicates that the voltage range used in the experiment offers a significant safety margin (Fig. 2). The computational model can also be adapted to explore other designs of tunable lenses, where mimicking human eyes may not be the object. For instance, in the design described in Ref. 37, a transparent conductor is used as electrodes, so that the dielectric elastomer actuator coincides with one side the lens, leading to a more compact device. In almost any design, many parameters can be varied, including the volume of the liquid, the refractive index of the liquid, the materials for the dielectric and the conductor, the prestretches of both sides of the lens, and the resting radii of the two sides of the lens. The computational model will enable the designer to explore the large parameter space to achieve the desired object and avert failure.

## VI. CONCLUDING REMARKS

We present a computational model of deformable lenses. The model predictions agree well with the reported experimental data. We show that the artificial muscle undergoes significantly inhomogeneous deformation, which may lead to failure by electrical breakdown and loss of tension at the outer boundary. The experiments carried out in Ref. 1, however, are well within the regime of safe operation. We use the model to calculate the characteristic curve of the performance of the lens, namely, the radius of curvature of the lens as a function of the voltage. The characteristic curve depends on a number of design parameters, including the prestretch, the volume of liquid, and the size of the dielectric elastomer actuator. We calculate how loss of tension and electrical breakdown limit the maximum absolute change and relative change of the radius of curvature. It is hoped that the computational model will aid the further development of deformable lenses.

## ACKNOWLEDGMENTS

This work was supported in Harvard by ARO (W911NF-09-1-0476), DARPA (W911NF-10-1-0113), and MRSEC (DMR-0820484). Lu was supported by China Scholarship Council as a visiting scholar for two years at Harvard University. Wang was supported by Zhejiang University through the Xinxing Plan and China Scholarship Council as a visiting scholar at Harvard University and by ZJNSFC (No. LY13A020001). Suo acknowledges a visiting appointment at The International Center for Applied Mechanics.

## APPENDIX A: EQUILIBRIUM EQUATIONS OF THE LENS

The equilibrium in the lens requires the work done by the liquid pressure $p\delta v$ equal to the change of the free energy of the lens $\delta F^l$. The free energy of the lens is

$$F^l = \int_0^A \pi H W_{stretch}(\lambda_1, \lambda_2) R dR. \tag{A1}$$

Upon loading pressure, the free energy changes as

$$\delta F^l = \pi H \int_0^A \left( \frac{\partial W_{stretch}(\lambda_1,\lambda_2)}{\partial \lambda_1} \delta\lambda_1 + \frac{\partial W_{stretch}(\lambda_1,\lambda_2)}{\partial \lambda_2} \delta\lambda_2 \right) R dR. \tag{A2}$$

Denote $s_1 = \frac{\partial W_{stretch}(\lambda_1,\lambda_2)}{\partial \lambda_1}$ and $s_2 = \frac{\partial W_{stretch}(\lambda_1,\lambda_2)}{\partial \lambda_2}$.

From Eqs. (1) and (2), we obtain the associated variation in the longitudinal stretch

$$\delta\lambda_1 = \frac{d\delta r}{dR}\cos\theta - \frac{d\delta z}{dR}\sin\theta, \tag{A3}$$

Inserting (A3) and $\delta\lambda_2 = \frac{\delta r}{R}$ into (A2), we obtain

$$\begin{aligned} \delta F^l &= \pi H \int_0^A \left( s_1 \cos\theta \frac{d\delta r}{dR} - s_1 \sin\theta \frac{d\delta z}{dR} + s_2 \frac{\delta r}{R} \right) R dR \\ &= \pi H (s_1 R \cos\theta \delta r)|_0^A - \pi H (s_1 \sin\theta R \delta z)|_0^A \\ &\quad + \pi H \int_0^A \left[ -\frac{d(s_1 R\cos\theta)}{dR}\delta r + \frac{d(s_2 R \sin\theta)}{dR}\delta z + s_2 \delta r \right] dR. \end{aligned} \tag{A4}$$

The work done by the liquid pressure is

$$\begin{aligned} p\delta v &= 2\pi p \int_0^A \left( r\frac{dr}{dR}\delta z + z\frac{dr}{dR}\delta r + zr\frac{d\delta r}{dR} \right) dR \\ &= 2\pi p (zr\delta r)|_0^A + 2\pi p \int_0^A \left( r\frac{dr}{dR}\delta z - r\frac{dz}{dR}\delta r \right) dR. \end{aligned} \tag{A5}$$

Equating $\delta F^l$ in (A4) to $p\delta v$ in (A5), we obtain the equilibrium equations

$$\frac{d}{dR}\left( \frac{H}{2} R s_1 \sin\theta \right) = \lambda_1 \lambda_2 R p \cos\theta, \tag{A6}$$

$$\frac{d}{dR}\left(\frac{H}{2}Rs_1\cos\theta\right)-\frac{H}{2}s_2=\lambda_1\lambda_2 Rp\sin\theta, \tag{A7}$$

and boundary conditions $\left(\frac{H}{2}Rs_1\cos\theta-pzr\right)\delta r|_0^A=0$

and $(s_1\sin\theta)\delta r|_0^A=0$. (A8)

## APPENDIX B: EQUILIBRIUM EQUATIONS OF THE DIELECTRIC ELASTOMER ACTUATOR

The equilibrium in the dielectric elastomer actuator requires the electrical work done by the battery $\Phi\delta Q$ equal to the change of the free energy of the dielectric elastomer actuator $\delta F^{II}$. The free energy of the dielectric elastomer actuator is

$$F^{II}=\int_A^B 2\pi HW(\lambda_1,\lambda_2,D)RdR. \tag{B1}$$

Upon electrical loading, the free energy changes as

$$\delta F^{II}=2\pi H\int_A^B\left(\frac{\partial W(\lambda_1,\lambda_2,D)}{\partial\lambda_1}\delta\lambda_1+\frac{\partial W(\lambda_1,\lambda_2,D)}{\partial\lambda_2}\delta\lambda_2+\frac{\partial W(\lambda_1,\lambda_2,D)}{\partial D}\delta D\right)RdR. \tag{B2}$$

Denote $s_1=\frac{\partial W(\lambda_1,\lambda_2,D)}{\partial\lambda_1}-\frac{\Phi}{H}D\lambda_2$ and $s_2=\frac{\partial W(\lambda_1,\lambda_2,D)}{\partial\lambda_2}-\frac{\Phi}{H}D\lambda_1$. Inserting $\delta\lambda_1=\frac{d\delta r}{dR}$ and $\delta\lambda_2=\frac{\delta r}{R}$ into (B2), we obtain

$$\begin{aligned}\delta F^{II}&=2\pi H\int_A^B\left[\left(s_1+\frac{\Phi}{H}D\lambda_2\right)\frac{d\delta r}{dR}+\left(s_2+\frac{\Phi}{H}D\lambda_1\right)\frac{\delta r}{R}+\frac{\partial W(\lambda_1,\lambda_2,D)}{\partial D}\delta D\right]RdR\\&=2\pi H\int_A^B\left[\left(\left[s_2-s_1+\frac{\Phi}{H}D(\lambda_1-\lambda_2)\right]/R-d\left(s_1+\frac{\Phi}{H}D\lambda_2\right)/dR\right)\delta r+\frac{\partial W(\lambda_1,\lambda_2,D)}{\partial D}\delta D\right]RdR\\&\quad+2\pi H\left[\left(s_1+\frac{\Phi}{H}D\lambda_2\right)R\delta r\right]\Big|_A^B.\end{aligned} \tag{B3}$$

The work done by the battery is

$$\begin{aligned}\Phi\delta Q&=2\pi\Phi\int_A^B\left(r\frac{dr}{dR}\delta D+D\frac{dr}{dR}\delta r+Dr\frac{d\delta r}{dR}\right)dR\\&=2\pi\Phi(Dr\delta r)|_A^B+2\pi\Phi\int_A^B\left(r\frac{dr}{dR}\delta D-r\frac{dD}{dR}\delta r\right)dR.\end{aligned} \tag{B4}$$

Equating $\delta F^{II}$ in (B3) to $\Phi\delta Q$ in (B4), we obtain the equilibrium equations

$$\frac{ds_1}{dR}-\frac{s_2-s_1}{R}=0, \tag{B5}$$

$$\frac{\partial W(\lambda_1,\lambda_2,D)}{\partial D}=\lambda_1\lambda_2\frac{\Phi}{H}, \tag{B6}$$

and boundary conditions $s_1\delta r|_A^B=0$. (B7)


[1]F. Carpi, G. Frediani, S. Turco, and D. D. Rossi, Adv. Funct. Mater. **21**, 4002 (2011).
[2]C. Friese, A. Werber, F. Krogmann, W. Mönch, and H. Zappe, IEE J. Trans. Electr. Electron. Eng. **2**, 232 (2007).
[3]L. Eldada, Rev. Sci. Instrum. **75**, 575 (2004).
[4]R. Pelrine, R. Kornbluh, Q. B. Pei, and J. Joseph, Science **287**, 836 (2000).
[5]F. Carpi, S. Bauer, and D. D. Rossi, Science **330**, 1759 (2010).
[6]P. Brochu and Q. B. Pei, Macromol. Rapid. Commun. **31**, 10 (2010).
[7]I. A. Anderson, T. A. Gisby, T. McKay, B. M. O'Brien, and E. Calius, J. Appl. Phys. **112**, 041101 (2012).
[8]Q. B. Pei, R. Pelrine, S. Stanford, R. Kornbluh, and M. Rosenthal, Syn. Met. **135**, 129 (2003).
[9]R. Shankar, T. K. Ghosh, and R. J. Spontak, Adv. Mater. **19**, 2218 (2007).
[10]G. Kovacs, L. Düring, S. Michel, and G. Terrasi, Sens. Actuators, A **155**, 299 (2009).
[11]S. Akbari and H. R. Shea, J. Micromech. Microeng. **22**, 045020 (2012).
[12]A. Cheng, WW-EAP Newsletter **13**, 2 (2011).
[13]T. Mckay, B. M. O'Brien, E. Calius, and I. A. Anderson, Appl. Phys. Lett. **97**, 062911 (2010).
[14]R. Kaltseis, C. Keplinger, R. Baumgartner, M. Kaltenbrunner, T. F. Li, P. Machler, R. Schwodiauer, Z. G. Suo, and S. Bauer, Appl. Phys. Lett. **99**, 162904 (2011).
[15]R. D. Kornbluh, R. Pelrine, H. Prahlad, A. Wong-Foy, B. McCoy, S. Kim, J. Eckerle, and T. Low, MRS Bull. **37**, 246 (2012).
[16]T. Q. Lu, J. S. Huang, C. Jordi, G. Kovacs, R. Huang, D. R. Clarke, and Z. G. Suo, Soft Matter **8**, 6167 (2012).
[17]M. Kollosche, J. Zhu, Z. G. Suo, and G. Kofod, Phys. Rev. E **85**, 051801 (2012).
[18]J. S. Huang, T. F. Li, C. C. Foo, J. Zhu, D. R. Clarke, and Z. G. Suo, Appl. Phys. Lett. **100**, 041911 (2012).
[19]C. Keplinger, T. F. Li, R. Baumgartner, Z. G. Suo, and S. Bauer, Soft Matter **8**, 285 (2012).
[20]S. J. A. Koh, T. F. Li, J. X. Zhou, X. H. Zhao, W. Hong, J. Zhu, and Z. G. Suo, J. Polym. Sci., Part B: Polym. Phys. **49**, 504 (2011).
[21]X. H. Zhao and Z. G. Suo, Phys. Rev. Lett. **104**, 178302 (2010).
[22]X. H. Zhao, W. Hong, and Z. G. Suo, Phys. Rev. B **76**, 134113 (2007).
[23]R. Huang and Z. G. Suo, Proc. R. Soc. A **468**, 1014 (2011).
[24]T. Q. Lu and Z. G. Suo, Acta Mech. Sin. **28**, 1106 (2012).
[25]Z. G. Suo, Acta Mech. Solida Sinica **23**, 549 (2010).
[26]A. N. Gent, Rubber Chem. Technol. **72**, 263 (1999).
[27]D. K. Vu, P. Steinmann, and G. Possart, Int. J. Numer. Methods Eng. **70**, 685 (2007).
[28]X. H. Zhao and Z. G. Suo, Appl. Phys. Lett. **93**, 251902 (2008).
[29]B. O'Brien, T. McKay, E. Calius, S. Xie, and I. Anderson, Appl. Phys. A **94**, 507 (2009).
[30]H. S. Park, Z. G. Suo, J. X. Zhou, and P. A. Klein, Int. J. Solids Struct. **49**, 2187 (2012).
[31]S. X. Qu and Z. G. Suo, Acta Mech. Solida Sinica **25**, 459 (2012).
[32]D. L. Henann, S. A. Chester, and K. Bertoldi, J. Mech. Phys. Solids **61**, 2047 (2013).
[33]N. Goulbourne, E. Mockensturm, and M. Frecker, J. Appl. Mech. Trans. ASME **72**, 899 (2005).
[34]T. H. He, X. H. Zhao, and Z. G. Suo, J. Appl. Phys. **106**, 083522 (2009).
[35]H. M. Wang, S. Q. Cai, F. Carpi, and Z. G. Suo, J. Appl. Mech. **79**, 031008 (2012).
[36]T. F. Li, C. Keplinger, R. Baumgartner, S. Bauer, W. Yang, and Z. G. Suo, J. Mech. Phys. Solids **61**, 611 (2013).
[37]S. Shian, R. M. Diebold, and D. R. Clarke, Opt. Express **21**, 8669 (2013).
[38]G. Kofod, R. Kornbluh, R. Pelrine, and P. S. Larsen, J. Intell. Mater. Syst. Struct. **14**, 787 (2003).